NDE of wood-based composites with longitudinal stress waves

1985 Wood Award Winner

Robert J. Ross
Roy F. Pellerin

Abstract

The research presented in this paper reveals that stress wave nondestructive testing techniques can be used to evaluate the tensile, flexural, and internal bond properties of wood-based composite materials. Results of preliminary tests conducted to explore stress wave behavior in these materials were enlightening. They indicated that wave speed and attenuation were material properties related to the same mechanisms that control these materials' mechanical behavior. For example, the tests revealed that wave attenuation, a parameter not previously explored or used in wood-based composite materials nondestructive testing programs, was related to bonding characteristics and, therefore, may contribute to the prediction of static properties. Results of an experimentation program designed to develop and explore mathematical relationships between stress wave characteristics and the static mechanical properties of wood-based composites verified preliminary findings. It was concluded that stress wave speed and attenuation could be used successfully to predict the static tensile and flexural properties of these materials. More importantly, it was possible to predict these properties at levels of accuracy previously considered unattainable. The developed regression models accounted for over 94 percent of these materials' observed elastic properties and for over 90 percent of their observed tensile and flexural strengths. Useful correlations for internal bond were also found.

Wood-based composite materials are manufactured by bonding wood elements together with an adhesive under elevated temperatures and pressures. Programs currently used to evaluate the quality of such materials require randomly removing a single full-sized panel from a production line, taking it into the laboratory, and destructively testing small sections sawn from it. When these tests are completed, the mechanical properties of that particular panel are fully known, but there is virtually no assurance that the next panel, or the next 100 panels, will have the same characteristics, good or bad. What is needed, therefore, is a quick and accurate nondestructive method of evaluating the mechanical properties of these materials.

Longitudinal stress wave nondestructive testing techniques show much promise for providing such an evaluation. These techniques use low stress molecular motions to measure two fundamental material properties: energy storage and dissipation. Energy storage is manifested as the speed at which a wave travels in a material. In contrast, the rate at which a wave attenuates is an indication of energy dissipation. Jayne (2) hypothesized that these properties are controlled by the same mechanisms that determine a material's mechanical behavior. As a consequence, useful mathematical relationships between stress wave and static mechanical properties should be attainable through statistical regression analysis techniques.

Early studies to verify this hypothesis were conducted with clear wood and lumber products. Jayne (2) was successful in demonstrating **a** relationship between energy storage and dissipation properties, measured by forced transverse vibration techniques, and the static bending properties of small, clear wood specimens. Pellerin (4) verified the hypothesis using free transverse vibration techniques and dimension lumber. Kaiserlik (3) furthered the hypothesis by using stress wave techniques to evaluate the tensile strength of a small sample of clear lumber containing varying degrees of slope of grain.

The authors are, respectively, Research Engineer, Research and Development, Trus Joist Corp., 501 E 45th St., Boise, ID 83714; and Professor, Civil and Environmental Engineering, Washington State Univ., Pullman, WA 99164. This paper was received for publication in February 1986.

Forest Prod. J. 38(5):39-45.

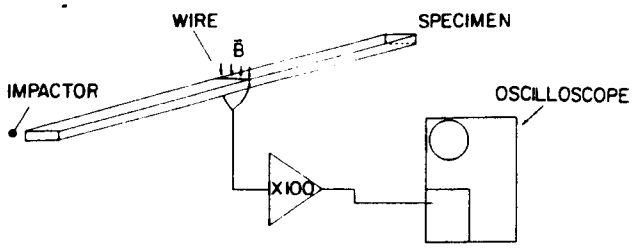

Figure 1. — Schematic diagram of the instrumentation used to observe stress wave behavior in several particle composite specimens.

Verification of Jayne's hypothesis using stress wave techniques on wood-based composite materials has been limited to studies that have employed only energy storage parameters in the prediction of mechanical properties of a limited spectrum of materials. Most encouraging was work done by Pellerin and Morschauser (5). They showed that stress wave speed could be successfully used to predict the flexural properties of underlayment particleboard. Wave attenuation and its contribution to the prediction of mechanical properties has not been investigated. This additional parameter may provide useful information about the mechanical behavior of wood-baaed composites because it is controlled by internal friction mechanisms to which bonding characteristics contribute significantly. In addition, due to the wide range and complex interaction of manufacturing parameters that combine to determine the mechanical properties of wood-based composites, it would be beneficial to test the validity of the hypothesis on a broad spectrum of composites.

The research reported herein dealt with the application of stress wave nondestructive testing techniques to wood-baaed composite materials. Its primary objective was to determine whether stress wave speed and attenuation characteristics could be used to evaluate the mechanical properties of these materials. A secondary objective was to explore stress wave behavior in wood-based composites.

Exploratory studies: stress wave behavior in wood-based composites

A series of experiments was conducted with several 3/4- by 6-inch by 4-foot specimens having widely different mechanical properties in order to gain insight into stress wave speed and attenuation behavior in wood-based composites. The experimental setup shown in Figure 1 was employed. Specimens were impacted at one end using a pendulum impactor. The impactor was fitted with a hardened steel ball approximately 7/8 inch in diameter and mounted in a small frame. Particle velocity of the midspan's cross section in response to the wave was observed and recorded using the instrumentation described by Ross (6).

Figure 2 shows oscilloscope traces obtained by monitoring the midspan particle velocity of the specimens. As expected from elementary wave theory, observed particle velocity was always in the same direction. Note that

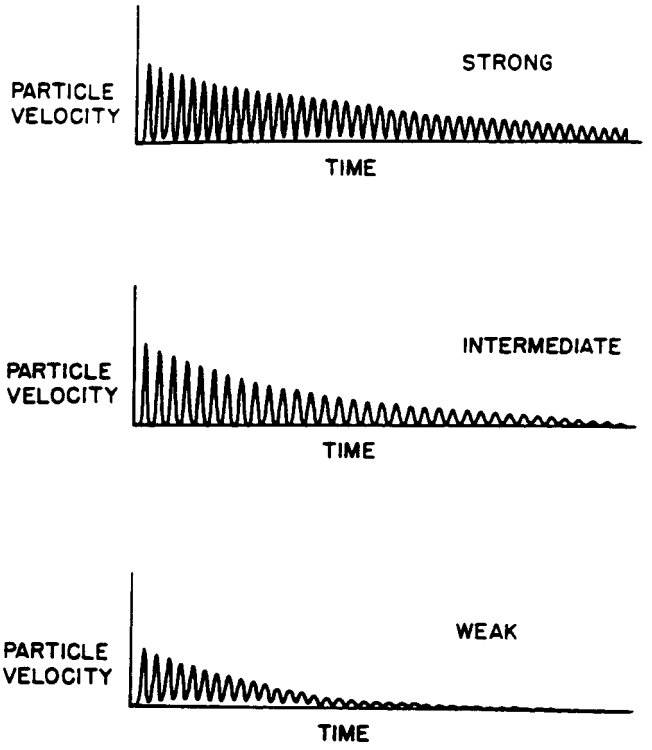

Figure 2. — Oscilloscope traces obtained by monitoring the particle velocity of the midspan cross section of several composite specimens.

the number of pulses per unit of time is determined by the speed at which a wave propagates back and forth in a specimen and that the rate at which particle velocity of a cross section decays is a measure of the attenuation of the wave (6). As evidenced by the number of pulses per unit time, wave speed was highest through the strong specimen and wave attenuation was greatest for the weak specimen.

It was interesting to note that specimens corresponding to the oscilloscope traces labeled intermediate and weak were both underpayment grade particleboard. The only difference between these two specimens was that the weak specimen was poorly bonded. Stress wave speed was found to be the same for both specimens while the rate of wave attenuation was greater for the weak specimen. This suggested that bonding characteristics do not dramatically affect the speed at which a wave travels, but do affect the rate at which a wave attenuates. This was verified by the results of a linear regression analysis comparing stress wave speed and attenuation characteristics to the static bending strengths of a sample of materials containing sound and poorly bonded specimens. Static bending rather than internal bond (IB) tests were performed so that the stress waved section could be destructively evaluated in its entirety. A coefficient of determination (R^2) value of 0.33 was obtained when stress wave speeds were compared to bending strength values. An R^2 value of 0.80 was obtained when the average rate of wave attenuation was correlated to bending strengths.

The results of these preliminary experiments were enlightening because they indicated that stress wave

speed and attenuation characteristics were properties related to the same mechanisms that control the mechanical behavior of wood-based composites. They also revealed that wave attenuation was an important nondestructive test parameter that might contribute significantly when used in the prediction of static mechanical properties. These encouraging results provided the impetus for the following experiments that were conducted to examine relationships between stress wave characteristics and the static mechanical properties of wood-based composites.

Materials and methods

A random sample of 160 2-foot by 8-foot wood-based composite panels that incorporated a wide range of static mechanical properties were obtained from several North American particleboard manufacturers. These commercial panels, whose characteristics are summarized in Table 1, were selected as being representative of the spectrum of panels currently produced by the North American particleboard industry. They were manufactured using various adhesive types, formulations and levels, wood species, and several widely varying particle geometries.

Upon arrival at Washington State University's Wood Engineering Laboratory, two 6-inch-wide specimens were cut from the larger panels, one each for static bending and tension tests. These specimens were then stickered and allowed to equilibrate at ambient conditions, which was approximately 6 percent equilibrium moisture content (EMC).

Stress wave behavior in each specimen was observed and recorded using the experimental setup described in the previous section. From this information, the average wave attenuation (ATT) and wave speed (C) were determined. Each specimen's weight, length, width, and thickness were recorded. Dynamic modulus of elasticity (MOE_d) was calculated using the simple formula, $MOE_d = C^2 p$.

Full size tension tests were conducted on the 6-inch by nominal 8-foot tension specimens using Washington State University's tension machine. A loading rate of 2,000 pounds per minute was used. Axial deformation of the specimens was measured using a linear variable differential transformer (LVDT) acting on a gauge length of 48 inches. From this information, elastic modulus was calculated based on the load at 0.10 inch deformation and actual cross-sectional dimensions. Ultimate tensile stress was computed from load at failure and actual cross-sectional dimensions.

Static bending tests were performed on specimens obtained from the 6-inch by nominal 8-foot sections using a Rhiele Universal Testing Machine. These tests were conducted according to ASTM D 1037-78 (1) standards with the following modifications. Specimens were loaded at their third points using a span-to-depth ratio of **36.** This resulted in a larger area over which the max-

TABLE 1. — *Representative commercial panel characteristics.*

Manufacturer	Board type	Particle orientation	Species	Raw material form	Raw material processing	Adhesive type	Intended end use
A	3-layer	Core layer particles 90° to the face layer particles	Aspen	Roundwood	Drum-flaker	Phenolic	Roof and floor sheathing
B	Homogeneous	Random	Mixture of white fir, pine, larch, and Douglas-fir	Planer shavings	Hammermill	Urea	Floor underlayment
C	Homogeneous	Random	Aspen	Roundwood	Disc-flaker	Phenolic	Roof and floor sheathing
D	Homogeneous	Maximum alignment	Aspen and balsam fir	Roundwood	Laboratory roundwood flaker	Isocyanate	High strength specialty products
E	3-layer	Core layer particles 90° to the face layer particles	Aspen	Roundwood	Disc-flaker	Phenolic	Roof and floor sheathing
F	3-layer	Random	80% Douglas-fir, 20% mixture of white fir and pine	30% green planer shavings, 20% dry-planer shavings, 25% sawdust, 25% plywood trim	Face: double disk refiner Core: ring flaker	Urea	Floor underlayment and furniture core stock
G	3-layer	Random	90% Douglas-fir, 10% hemlock, white fir	75 to 80% planer shavings, 20 to 25% plywood trim	Attrition mill	Urea	Floor underlayment
H	3-layer	Random	Southern pine	Dry-planer shavings	Single disk refiner	Urea	Furniture core stock

imum bending moment would be applied as compared to that of a centerpoint loading setup. In addition, this center region would not be subjected to shear stresses as would be the case of a specimen loaded at its midspan. In order to maintain a constant span-to-depth ratio, the length of specimens obtained for each 6-inch wide section varied as shown in Table 2. A specimen width of 6 inches was used instead of the required width of 3 inches in an effort to reduce test result variability that may result from small specimen sizes.

Using an LVDT deflection measuring system, load versus midspan deflection was continuously recorded. From this information, elastic modulus was calculated. Modulus of rupture (MOR) was calculated from load at failure and actual cross-sectional dimensions.

Two 6- by 6-inch IB specimens were obtained from the previously tested tension specimens. This size was used instead of the 2- by 2-inch required size in an effort to reduce test result variability which might result from small specimen sizes.

All IB specimens were tested to failure using a Rhiele Universal Testing Machine. Loading rates were applied as specified by ASTM Standard D 1037-78. Load at failure was recorded for each specimen, together with failure location.

Univariable and multivariable linear regression analyses were used to examine the relationships between measured nondestructive parameters and the tensile, flexural, and IB properties of the material tested. Nondestructive parameters included specific gravity (SG), wave speed (C), dynamic modulus of elasticity (MOE_d), and wave attenuation (ATT).

The mathematical regression equations used in this analysis were assumed to be of the following form:

$$P = KN_0^x N_1^y N_2^z \quad [1]$$

TABLE 2. — *Number, length, and span length of bending specimens obtained from 6-inch by nominal 8-foot sections.*

Nominal panel thickness	Number of specimens	Specimen length	Span length
(in.)		(in.)	
1/2	4	20	18
5/8	4	23	21
3/4	3	28	27
1	2	38	36

where:

P = property being estimated
K, x, y, and z = empirical constants
N_0, N_1, and N_2 = nondestructive parameters

A linear regression analysis of the data was used to determine values for K, x, y, and z. This was accomplished by first taking the natural logarithm of Equation [1], which resulted in the following:

$$\ln(P) = \ln(K) + x \ln(N_0) + y \ln(N_1) + z \ln(N_2) \quad [2]$$

The coefficients and constants in Equation [1] were determined with the aid of a computer using matrix algebra and multiple linear regression analysis techniques. The coefficients obtained were then substituted into Equation [1] and an estimated value of each property teated was obtained using measured nondestructive parameters. A linear regression analysis of estimated versus actual values was then performed to determine how well each parameter estimated a particular property.

Results and discussion

Tensile and flexural modulus of elasticity

Results obtained from the various regression analyses are summarized in Table 3. Correlation coefficients *(R)* obtained from these analyses indicated that SG is a poor predictor of either tensile or flexural moduli. The developed regression models, using SG as a predictor, accounted for less than 1 percent of the materials' observed behavior.

A strong correlation existed between stress wave speed and tensile and flexural static moduli. The developed model accounted for 96 percent of the materials' observed tensile behavior and 94 percent of observed flexural behavior.

Figures 3 and 4 show plots of tensile and flexural moduli, predicted using MOE_d, versus actual values. Because of the wide range of properties observed, predicted and actual values were plotted on logarithmic scales. These plots show that strong relationships existed between MOE_d and static moduli values. The developed regression models accounted for over 93 percent of the materials' observed behavior.

TABLE 3. — *Results of linear regression analyses relating static tensile and flexural elastic moduli, ultimate tensile stress, and modulus of rupture to nondestructive parameters. The coefficients K and x are used in the generalized mathematical model: ln (property) = ln (K) + x ln (N_o).*

Predictor	Tensile modulus of elasticity				Flexural modulus of elasticity			
	ln(K)	x	R[a]	S_{yx}[b]	ln(K)	x	R[a]	S_{yx}[b]
Specific gravity (SG)	−0.944	−0.580	0.11	0.484	−0.867	−0.515	0.11	0.446
Wave speed squared (C^2)	−18.636	1.000	0.98	0.100	−16.746	0.899	0.97	0.135
Dynamic modulus of elasticity (MOE_d)	−0.130	1.018	0.98	0.106	−0.109	0.934	0.96	0.122
	Ultimate tensile stress				Modulus of rupture			
Specific gravity (SG)	7.319	−0.338	0.07	0.447	7.854	0.164	0.07	0.460
Attenuation (ATT)	11.353	−1.306	0.63	0.347	12.198	−1.362	0.70	0.328
Wave speed squared (C^2)	−8.090	0.855	0.91	0.187	−7.891	0.878	0.93	0.193
Dynamic modulus of elasticity (MOE_d)	7.739	0.905	0.93	0.150	8.321	1.211	0.92	0.155

[a] Correlation coefficient.
[b] Standard error of estimate.

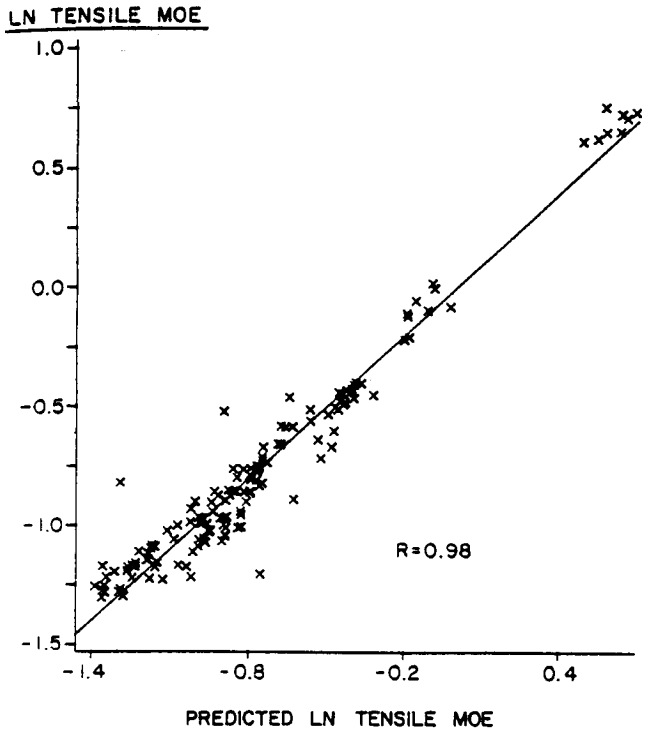

Figure 3. — Plot of tensile MOE, predicted using the dynamic MOE (MOE_d), versus actual tensile MOE values.

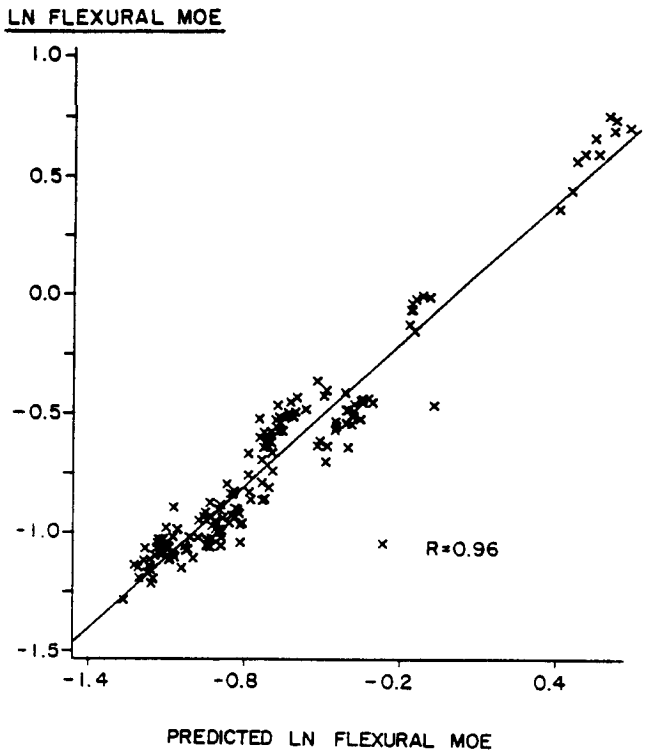

Figure 4. — Plot of flexural MOE, predicted using the dynamic MOE (MOE_d), versus actual flexural modulus values.

Ultimate tensile stress and modulus of rupture

Constants for the equations and *R* values obtained from the regression analyses are summarized in Table 3. *R* values indicated that SG was a poor predictor of either ultimate tensile stress or modulus of rupture (MOR). The developed regression models, using SG as a predictor, accounted for less then 1 percent of the materials' observed behavior.

Results obtained from the linear regression analyses revealed that the developed regression models relating ATT to ultimate stress values were statistically significant. *R* values showed that these models accounted for approximately 40 to 50 percent of observed behavior.

Plots of ultimate tensile stress and MOR values, predicted using MOE_d, versus actual values are shown in Figures 5 and 6. Values obtained from the linear regression analyses revealed that MOE_d was a better predictor of ultimate tensile stress and MOR than C. Since MOE_d is a function of C and SG. this shows that although SG was a poor predictor of these properties, it had an interactive effect that contributed significantly when used in conjunction with C.

In an effort to obtain a better prediction model for ultimate tensile stress and MOR, a multivariable regression model relating these properties to SG, ATT, and C was developed. Results of the regression analyses and values for the constants in the equations are summarized in Table 4.

A plot of ultimate tensile stress, predicted using the developed multivariable model, versus actual ultimate

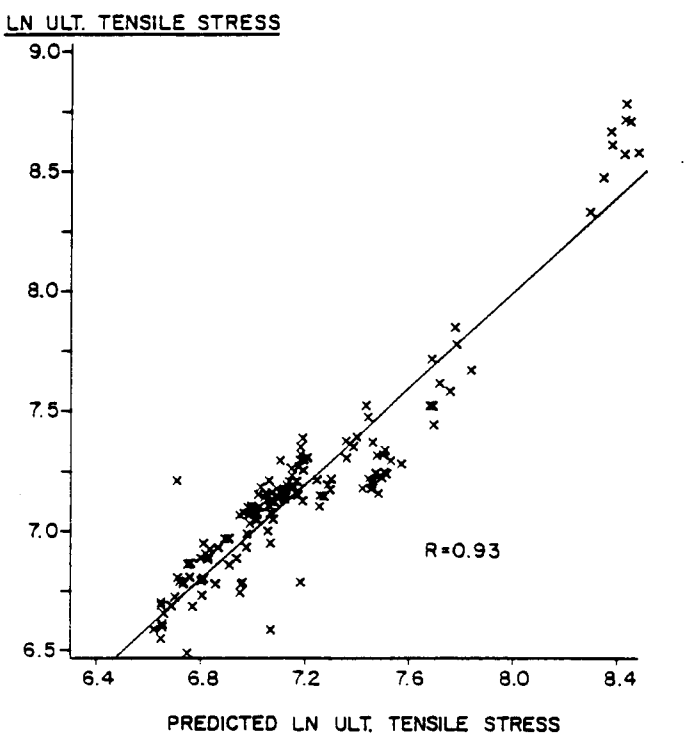

Figure 5. — Plot of ultimate tensile stress, predicted using the dynamic MOE (MOE_d), versus actual values.

tensile stress values is shown in Figure 7. This plot shows that a strong correlation existed between predicted and actual values. Results of the linear regression analysis revealed that approximately 90 percent of the materials' observed behavior was accounted for by the developed model. This showed that the multivariable model was a better predictor of ultimate tensile stress than MOE_d because the regression model developed utilizing MOE_d accounted for only 88 percent of the materials' observed behavior. Also, the standard error of estimate (S_{yx}) was approximately 6 percent smaller than the value obtained utilizing MOE_d as a predictor.

It is important to note that the exponent corresponding to ATT was found to be negative. This was expected because stronger boards would have smaller ATT values than weaker boards.

A plot of MOR, predicted using the multivariable model, versus actual MOR values is shown in Figure 8. The plot shows that a strong relationship existed between predicted and actual values. Results of the linear regression analysis revealed that 94 percent of the materials' observed behavior was accounted for by the multivariable model, whereas the model developed utilizing MOE_d accounted for only 88 percent of observed behavior. This information, plus the fact that S_{yx} was approximately 16 percent smaller for this model than that obtained using MOE_d as a predictor, showed that the multivariable model was a much better predictor of MOR.

Mathematical regression models relating the various nondestructive parameters and IB values of specimens taken from structural flakeboard materials were

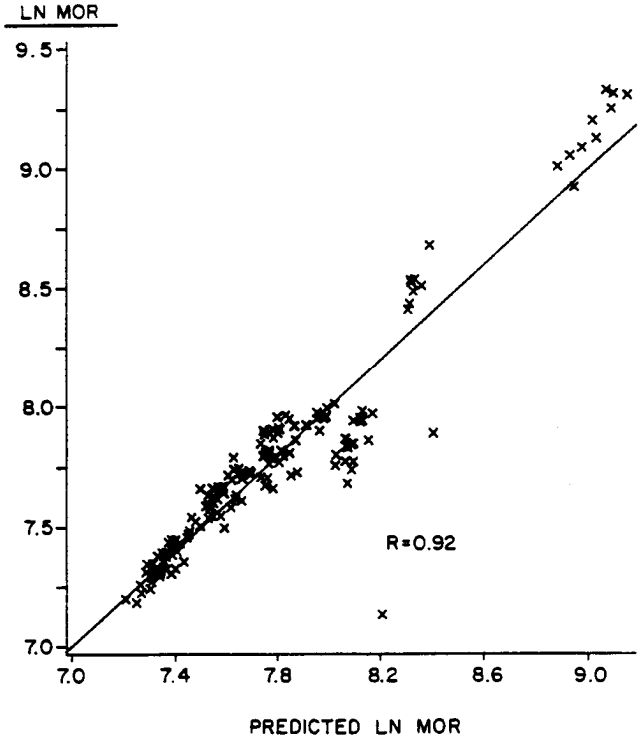

Figure 6. — Plot of MOR, predicted using the dynamic MOE (MOE_d), versus actual values.

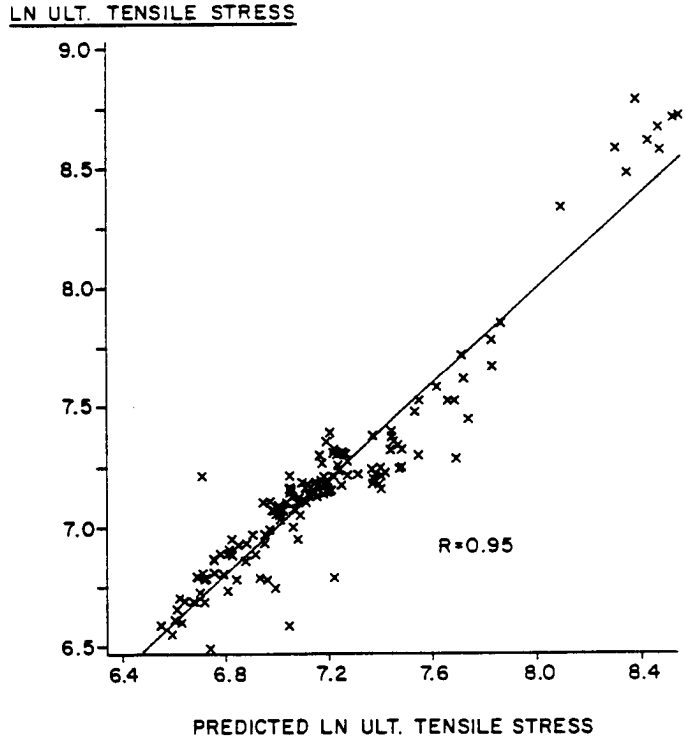

Figure 7. — Plot of ultimate tensile stress, predicted by a multivariable model utilizing wave speed, attenuation, and specific gravity, versus actual values.

TABLE 4. — *Results of a linear regression analysis relating ultimate tensile stress to the multiparameter regression model: ln (ultimate tensile stress or MOR) = ln (K) + x ln (SG) + y ln (ATT) + z ln (C^2).*

	Ultimate tensile stress					
Predictor	ln (*K*)	*x*	*y*	*z*	R^a	$S_{yx}{}^b$
ln ultimate tensile stress = ln (*K*) + *x* ln (*SG*) + *y* ln (*ATT*) + *z* ln (C^2)	−5.822	1.461	−0.312	0.812	0.95	0.140
	MOR					
Predictor	ln (*K*)	*x*	*y*	*z*	R^a	$S_{yx}{}^b$
ln MOR = ln (*K*) + *x* ln (*SG*) + *y* ln (*ATT*) + *z* ln (C^2)	−3.642	1.780	−0.518	0.769	0.97	0.130

[a] Correlation coefficient.
[b] Standard error of estimate.

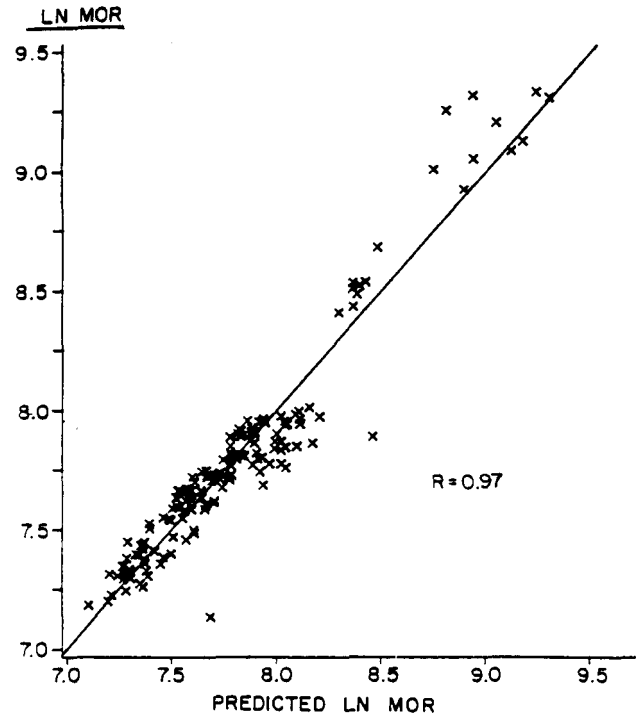

Figure 8. — Plot of MOR, predicted by a multivariable model utilizing wave speed, attenuation, and specific gravity, versus actual values.

assumed to be of the same form as Equations [1] and [2]. Results of linear regression analyses revealed useful relationships between predicted and actual values. A correlation coefficient of 0.80 was found when the three-parameter combination model incorporating SG, ATT, and C was used to predict IB values. Stronger relationships would be expected if IB specimens were taken along the entire length of the stress-waved section, as a section may contain areas of both high and low quality material. The information obtained from the nondestructive evaluation yielded average values for an entire stress-waved section. IB specimens were not taken along the entire section and, therefore, it was possible that average stress wave characteristics were compared with IB values for specimens taken from only high or low quality areas.

Conclusions

Based on the results of these experiments, it can be concluded that stress wave speed and attenuation characteristics are related to the same mechanisms that control the mechanical properties of wood-baaed composite materials because they were strongly correlated to static properties. More important, however, is the fact that these nondestructive testing parameters allow for the prediction of static mechanical properties at levels of accuracy previously considered unattainable. The developed regression models accounted for 94 percent of observed elastic behavior and for over 90 percent of observed tensile and flexural strengths. Strong correlations with IB properties were also found.

Literature cited

1. American Society for Testing and Materials. 1984. Annual Book of ASTM Standards. Part 22, D 1037. Philadelphia, Pa.
2. Jayne, B.A. 1959. Vibrational properties of wood as indices of quality. Forest Prod. J. 9(11):413-416.
3. Kaiserlik, J.H. 1975. Attenuation of stress waves as an indicator of lumber strength. M.S. thesis. Washington State Univ., Pullman, Wash.
4. Pellerin, R.F. 1965. A vibrational approach to nondestructive testing of structural lumber. Forest Prod. J. 15(3):93-101.
5. _____ and C.R. Morschauser. 1974. Nondestructive testing of particleboard. *In*: Proc. Seventh Particleboard Symposium. Washington State Univ., Pullman, Wash. pp. 251-260.
6. Ross, R.J. 1984. Stress wave speed and attenuation as predictors of the tensile and flexural properties of wood-based particle composites. Ph.D. diss. Washington State Univ., Pullman, Wash.